

Quantitative landslide hazard assessment along a transportation corridor in southern India

Pankaj Jaiswal^{a,b,*}, Cees J. van Westen^b, Victor Jetten^b

^a Geological Survey of India, Bandlaguda, Hyderabad, Andhra Pradesh, India

^b International Institute for Geo-Information Science and Earth Observation (ITC), Hengelosestraat 99, 7500 AA, Enschede, The Netherlands

ARTICLE INFO

Article history:

Received 19 June 2009

Received in revised form 7 September 2010

Accepted 7 September 2010

Available online 16 September 2010

Keywords:

Landslide

Spatial probability

Temporal probability

Magnitude probability

Validation

Nilgiri Hill

ABSTRACT

A quantitative model for landslide hazard assessment on natural slopes is presented for a transportation corridor of the Nilgiri Hills in southern India. The data required for the hazard assessment were mostly obtained from historical records. For the hazard modeling, a landslide inventory map was prepared from technical reports and maintenance records for a road and a railroad, available for a 21 year period from 1987 to 2007. Most landslides are shallow translational debris slides and debris flow slides triggered by rainfall. On natural slopes landslides occurred as first-time failures.

A logistic regression model was used to determine the spatial probability of landslides for each pixel by taking the source area of the existing landslides as dependent, and slope angle, aspect, regolith thickness and land use as independent variables. The temporal probability of landslides was estimated indirectly using the exceedance probability of the rainfall threshold required to trigger landslides for the first time on natural slopes. The probability of landslide size was estimated as frequency percentage of landslide volume, a proxy for landslide magnitude, and the percentage values were then expressed as probability. By assuming independence among the three probabilities, a quantitative estimate of a landslide hazard was obtained as the joint probability of landslide volume, of landslide occurrence in an established time period and of spatial probability of a landslide initiation. The models were validated using the rainfall and landslide events that occurred during 2008 and 2009.

Total 12 specific landslide hazard maps were generated considering six time periods (1, 3, 5, 15, 25 and 50 years), and two landslide volumes (volume exceeding 1000 m³ and 10,000 m³).

© 2010 Elsevier B.V. All rights reserved.

1. Introduction

Landslide hazard is defined as the probability of occurrence of a potentially damaging landslide within a specified period of time and within a given area (Varnes, 1984). According to the guidelines given by JTC-1, the Joint Technical Committee on landslides and Engineered Slopes (Fell et al., 2008), a quantitative landslide hazard map at a catchment scale should include their classification, volume (or area), location and velocity of potential landslides, and probability of their occurrence.

For landslides on natural slopes, the JTC-1 guidelines recommended using hazard descriptor as the annual probability of active landsliding for individual landslides and the number of landslides per unit area for small landslides on natural slopes. The JTC-1 guidelines also recommend carrying out hazard assessment according to the landslide type and magnitude. Due to the lack of well established

classification systems for landslide magnitude (Guzzetti et al., 2002), some researchers have used landslide area or volume as a proxy for magnitude for certain landslide types such as slides or flows (Guzzetti et al., 2005). In probabilistic terms, Guzzetti et al. (2005) included landslide area, which is considered a proxy for landslide magnitude, in the hazard assessment and calculated hazard as the joint probability of landslide size (area), of landslide occurrence in an established time period and of landslide spatial occurrence given the local environmental setting. The probabilistic model fulfils the definition of landslide hazard given by Varnes (1984), amended by Guzzetti et al. (1999) to include the magnitude of the landslide. Although one could argue this expression of landslide hazard as it assumes that the spatial probability, temporal probability and size probability are independent, it is currently the best applicable method for landslide hazard assessment at a medium scale (1:25,000–1:50,000). Other probabilistic methods that are based on process based modeling, experience serious problems with parameterization, which makes their application problematic over larger areas, especially in a heterogeneous terrain setting (Kuriakose et al., 2009a).

For estimating the susceptibility, or spatial probability of landslide occurrence, numerous models are available that have been

* Corresponding author. International Institute for Geo-Information Science and Earth Observation (ITC), Hengelosestraat 99, 7500 AA, Enschede, The Netherlands. Tel.: +31 53 4874 512; fax: +31 53 4874 336.

E-mail address: jaiswal@itc.nl (P. Jaiswal).

successfully used (e.g., Soeters and van Westen, 1996; Chung and Fabbri, 1999; Guzzetti et al., 2005; Lee and Pradhan, 2006). On the contrary, the number of publications on landslide hazard assessment at the catchment scale is still rather modest, due to the difficulty to add the temporal dimension to susceptibility maps at this scale. But, recently few progresses have been made to produce real hazard maps by incorporating temporal probability (e.g., Zezere et al., 2004; Guzzetti et al., 2005; Harp et al., 2009).

The temporal probability of landslides can be estimated from past landslide records using a Poisson or Binomial distribution model assuming that the rate of occurrence of landslides would remain the same (e.g., Lips and Wiczorek, 1990; Coe et al., 2000; Guzzetti et al., 2002, 2005). The model provides the probability of getting one or more landslides at any given time. The statistics involved are simple and results are easy to implement, but the main limitation is that it requires a sufficiently complete landslide inventory of multiple periods to compute probability. Also methods based on recurrences of past landslides are valid for the repetitive events and do not hold true for the unique ones (Guzzetti et al., 1999; Cascini et al., 2005). Furthermore, the temporal probability based on the mean rate of slope failures provides probability values to areas (e.g., a slope unit) that have experienced landslides and the areas with no record of past slope failures are classified as hazard free. Some researchers have used the frequency of occurrence of landslide triggers to estimate the temporal probability of landslides (e.g., Crozier, 1999; Chleborad et al., 2006). The advantage of this method is that it does not require a complete multi-temporal landslide inventory but, it is necessary here to establish reliable relations between the trigger, its magnitude and the occurrence of landslides. The method helps to model the temporal probability of first-time slope failures by determining the magnitude of trigger that has resulted in a slope to fail for the first time (Jaiswal and van Westen, 2009). Since the frequency of the trigger itself does not provide information on the spatial distribution of potential landslides, it has to be combined with landslide susceptibility to produce a landslide hazard map (Corominas and Moya, 2008). One way to overcome this and provide a combined spatial and temporal probability would be to carry out a statistical analysis using a substantially complete event-based landslide inventory, an inventory of landslides caused by the same triggering event, and use the return period of the trigger as the temporal probability (e.g., Glade, 2001). However, complete event-based landslide inventories are difficult to obtain either through traditional photo-interpretation techniques, with the common problem of linking them to particular dates of occurrence (van Westen et al., 2006) or from historical landslide records, which often report only those landslides that have caused damage (Guzzetti et al., 1994; Chau et al., 2004; Devoli et al., 2007).

In this paper, we propose a landslide probabilistic model to quantify hazard of first-time slope failures on natural slopes using the frequency of the landslide trigger. We calculated landslide hazard as the joint probability of landslide size (volume), of landslide occurrence in an established time period and of landslide spatial occurrence given the local environmental setting, based on an earlier work presented by Guzzetti et al. (2005). The required data for hazard analysis were obtained from the historical records available for the study area.

2. The study area

The study area is a transportation corridor in part of the Nilgiri Hills, in the western Tamilnadu region of southern India (Figure 1). The area covers 22 km² and forms a part of the Coonoor river basin with Tiger Hill–Kori Betta Ridge to the North and Coonoor River to the South.

Geologically, the area exposes charnockite rocks and garnetiferous quartzofelspathic gneisses belonging to the Charnockite Group of Archaean age (Seshagiri and Badrinarayanan, 1982). These are overlain by soil and laterite. The charnockite is also garnetiferous

and outcrops are well exposed along cut slopes of the road, railroad and landslide scarps. The regional strike of the foliation is ranging from ENE–WSW to E–W directions with moderate to steep dips. The sub-tropical climate and intense physical and chemical weathering have resulted in a thick yellowish to reddish brown soil. The regolith thickness varies from less than a meter to 20 m, as observed in cut slopes along the road and railroad.

Tea plantations form the main land use type, and on the steeper slopes there are many patches of forest. The settlements are very few and sparse, and only Burliyar and Katteri are the two major commercial and residential settlements along the road whereas other residential units are within tea estates.

The area experiences rainfall in two periods: April to July and September to December, of which November is the wettest month. During the period from 2002 to 2006, the annual rainfall in the area ranged from 836 mm to 3165 mm, with an average value of 1724 mm and a standard deviation of 330 mm. The average annual rainfall is lowest around Carolina area (974 mm) and highest around Katteri farm (2231 mm) (Figure 2).

3. Landslide inventory

An inventory map for landslides on natural slopes was prepared from the historical records and field observation. The historical records include technical reports on landslide investigations undertaken in the study area during a 21 year period from 1987 to 2007. The technical reports provided a detailed description of landslide location, detail maps and field photographs of some of the landslides, and other parameters such as landslide morphometry, date of occurrence, volume, etc. The historical records were thoroughly studied and relevant information pertaining to landslides in the area was compiled. After compilation, field work was carried out to locate the landslides on the basis of description given in the reports. The data on landslide volume was used to infer the size of landslides and the morphological signatures left by landslides on slopes such as barren slopes, scarp faces, etc. were used to identify the shape of landslides. The morphological parameters (landslide scar length, width and depth) were plotted after carefully measuring them in the field using a meter tape. For landslides located on inaccessible slopes the morphological parameters were plotted based on the field observation, image interpretation and description given in technical reports. The availability of detailed maps and field photographs of some landslides on natural slopes facilitated in identifying the shape of landslide scars and run-out areas. The volume and area of mapped landslides was recalculated by multiplying the morphological parameters.

After identifying the exact location of landslides on hill slopes, they were then mapped on a 1:10,000 scale topographic map. Their initiation (source) and run-out area were separately marked. The landslides were digitized in a GIS environment. The coordinates were obtained through GIS and other details were attached as an attribute table.

Substantially complete information from technical reports was available only for landslides triggered by a rainfall event on 14 November 2006. All landslides triggered by this event were systematically recorded, including those affecting cut slopes. In 2007, we carried out a field work and updated the 2006 inventory, and also included landslides that have occurred in uninhabited areas.

Fig. 3 shows the distribution of mapped landslides on natural slopes. A total of 31 landslides have been identified, which are either classified as translational debris slides (Figure 4A) or debris flow slides (Figure 4B–D). All occurred as first-time failures, and were triggered by rainfall. The landslides in natural slopes are generally small in size (with a landslide source area ranging from 60 to 15,000 m²), but known to have resulted in numerous casualties and losses to properties, including houses, tea plants and horticulture. In 1993, a large debris flow slide at Marapallam (Figure 4B) killed more

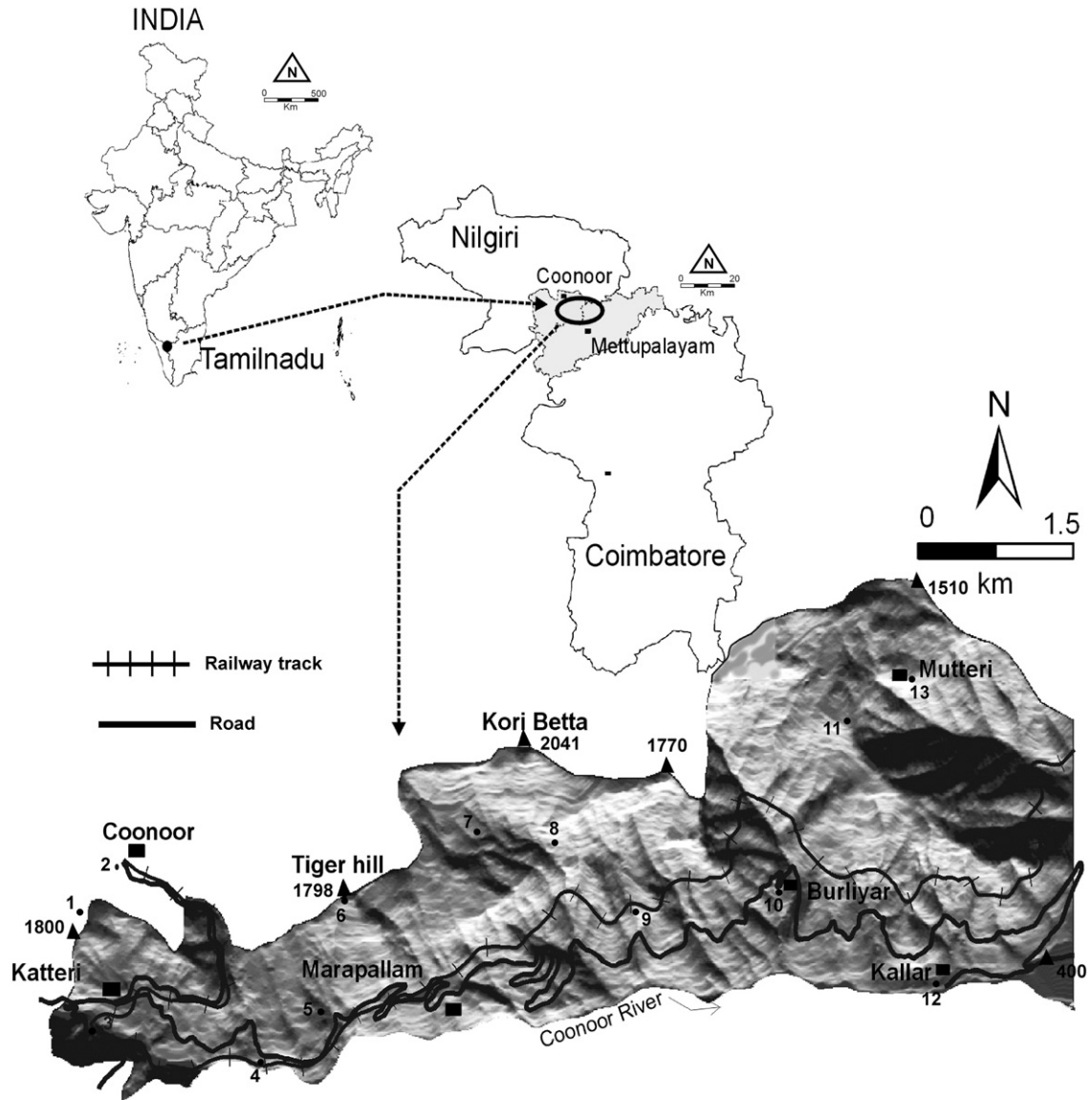


Fig. 1. Location map of the study area. Black triangles indicate spot height (in meters) above the mean sea level. Black circles are the location of rain gauge stations: 1 – Carolina (Car), 2 – Coonoor (Coo), 3 – Glandale (Gla), 4 – Runnymede (Run), 5 – Katteri farm (Kat), 6 – Tiger Hill (Tig), 7 – Singara upper division (SinUD), 8 – Singara lower division (SinLD), 9 – Hillgrove (Hil), 10 – Burliyar (Bur), 11 – Adderley (Add), 12 – Kallar farm (Kal), and 13 – Mutteri (Mut).

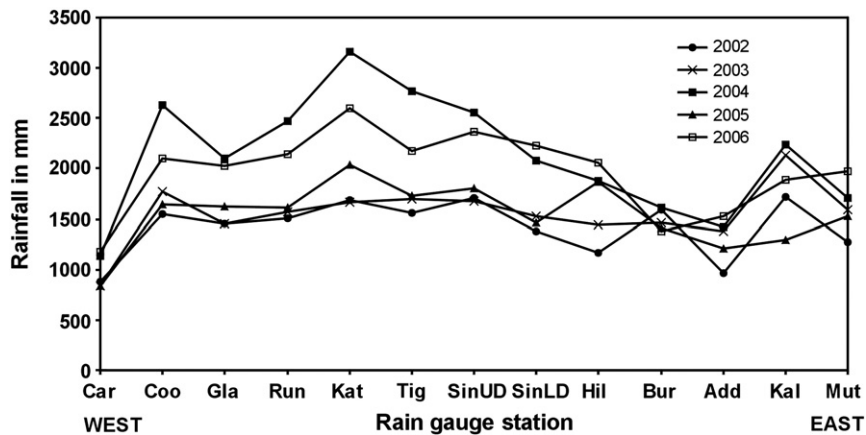


Fig. 2. Annual rainfall values at different rain gauges. The names of the rain gauge stations are shown in abbreviated form on the x-axis (see description of Figure 1 for the full name). ‘Car’ is located to the western and ‘Mut’ in the eastern boundary of the study area.

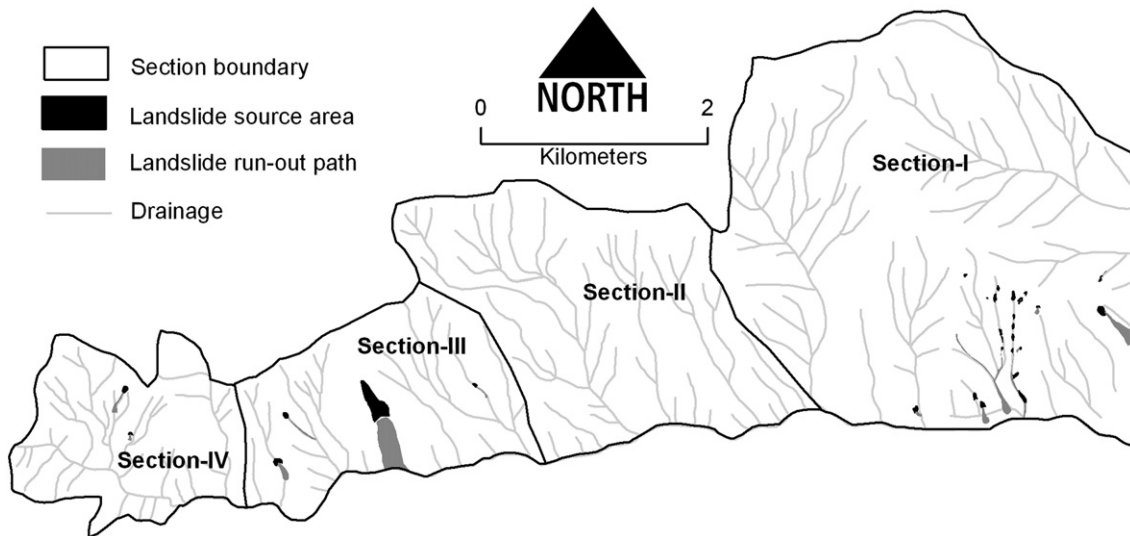


Fig. 3. Location of landslide source and run-out areas on natural slopes. Sections I, II, III and IV are the areas used for determining rainfall thresholds.

than 50 people, and destroyed 18 houses and one mosque (Balachandran et al., 1996). On 14 November 2006, a debris flow slide east of Kallar farm (Figure 4D) destroyed part of the horticulture property. Fig. 4C shows the crown portion of the debris flow slide near Kallar farm.

During the period 1987 to 2007, rainfall has triggered landslides on seven occasions on natural slopes. For example, on 14 November 2006 about 150 mm of rainfall in 3 h has triggered 166 landslides around Burliyar. The 2006 rainfall event has triggered landslides both on natural slopes and on cut slopes along the transportation lines.

4. Method for landslide hazard assessment

A quantitative landslide hazard assessment on natural slopes requires the estimation of three basic parameters (Figure 5):

- (1) the magnitude probability (P_M), indicating the probability that the landslide might be of a given size,
- (2) the temporal probability (P_T): indicating the annual probability of occurrence of triggering events that generate landslides, and

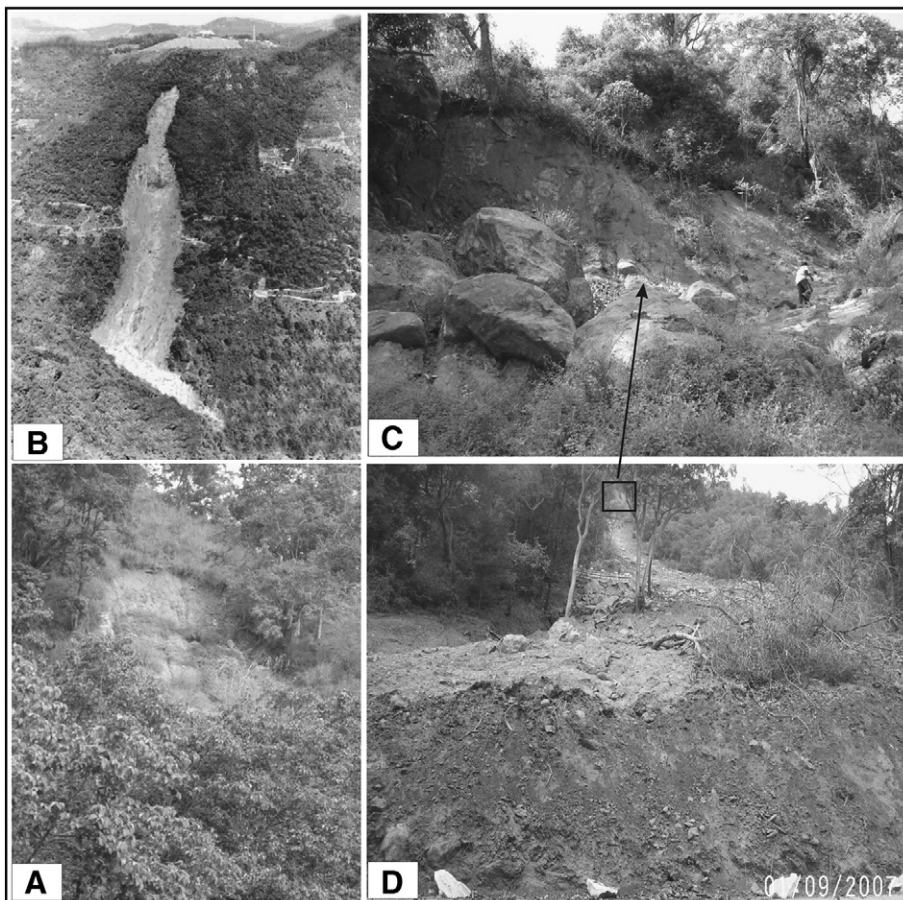


Fig. 4. Examples of landslides on natural slopes in the study area. Landslides are debris slides (A) and debris flow slides (B–D) triggered by rainfall as first-time failures.

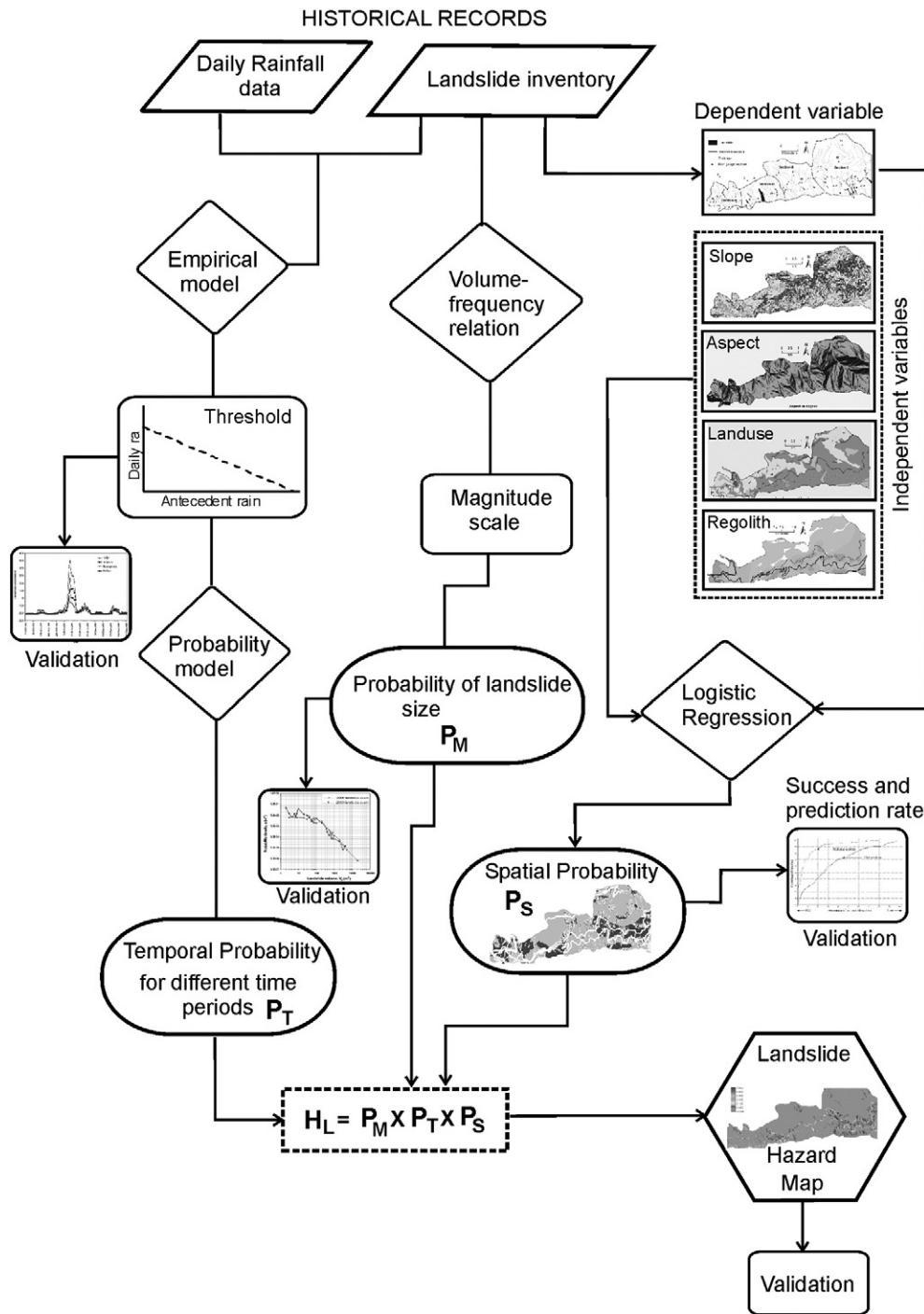


Fig. 5. Parameters and process adopted for the quantitative assessment of landslide hazard.

(3) the spatial probability (P_S): indicating the relative spatial probability of occurrence of landslides of a given type.

Using the above probabilities, the landslide hazard on natural slopes can be estimated as the joint probability of the landslide size, of the landslide occurrence in an established time period and of the landslide spatial occurrence (Guzzetti et al., 2005). It is assumed that the above three probabilities are mutually independent and the landslide hazard (H_L), i.e., the joint probability is:

$$H_L = P_M \times P_T \times P_S \quad (1)$$

The assumption that the three probabilities in Eq. (1) are mutually independent may not hold always and everywhere. Small triggering

events will result in another landslide magnitude distribution than a large triggering event, and also the locations where landslides will occur may be substantially different. However, the assumption is accepted here as the best approach given the lack of a better approach that can be used under the given circumstances of data availability and characteristics of the study area. In areas where a complete landslide inventory is available (e.g., inventory available for Hong Kong Island) attempts have been made to zone landslide hazard directly using the number of landslides per year per mapping unit (Chau et al., 2004). However, such method requires a complete multi-temporal landslide inventory, which is seldom available.

The assessment of landslide hazard on cut slopes will be taken up separately because the mechanism and processes involved in

initiating slope failures on cut slopes are different than on the natural slopes. Slope failures on cut slopes are mainly due to the effect of anthropogenic interference, which makes slopes conducive for landslides to initiate.

5. Probability of landslide size (volume)

To ascertain the probability of the landslide volume, we selected 166 landslides triggered by the November 2006 landslide event because of the availability of a substantially complete record. We use the term ‘landslide event’ for those days for which one or more landslides were triggered by rainfall. For the analysis, we used the volume estimated at the source of landslides. Out of the 166 landslides triggered by the 2006 event, 18 occurred on natural slopes and the rest on cut slopes. Most landslides on natural slopes had a volume less than 1000 m³ and occurred on steep slopes (Figure 4A). Only 4 landslides had a volume larger than 1000 m³.

To ascertain the probability, we first studied the probability density distribution of landslide volume of the 166 landslides obtained using the equation given in Malamud et al. (2004). The probability density $p(V_L)$ is expressed as:

$$p(V_L) = \frac{1}{N_{LT}} \frac{\delta N_L}{\delta V_L} \tag{2}$$

where δN_L is the number of landslides with volumes between V_L and $V_L + \delta V_L$, and N_{LT} is the total number of landslides.

Fig. 6 shows the probability density distribution of the landslide volume. The observed probability density distribution shows distinct flattening of the curve (roll-over) for failure volumes of less than 200 m³.

In most studies, the relationship of the landslide size and frequency is observed to have a power law distribution over two orders of landslide size with a flattening of curve at the lower size (e.g., Stark and Hovius, 2001; Guthrie and Evans, 2004; Malamud et al., 2004). Researchers have studied the frequency distribution using different types of landslide inventories, as mentioned in Picarelli et al. (2005). These examples include inventories containing landslides for an undefined long period of time prior to a mapping timeline, inventories of landslides within a defined time interval, inventories containing continuous records of landslide occurrence within a region or along transportation corridors, and inventories of landslides

occurring in a very short period of time after a triggering event such as an earthquake or rainstorm. Some researchers (e.g., Guthrie and Evans, 2004) believe that the flattening of the curve at the lower landslide size is ‘natural’ and reflects slope stability processes whereas others (e.g., Chau et al., 2004; Malamud et al., 2004; Catani et al., 2005) relate it to the incompleteness of the inventory. Brardinoni and Church (2004) have shown an increase in the frequency of small landslides when the photo-interpreted inventory was integrated with an intensive field based inventory.

The actual frequency distribution of landslide size, thus remains unclear in literature and also in the study area due to the lack of complete records for other events and the unavailability of an established model for landslide size and frequency for the Nilgiri Hills. In this study, we computed the probability of landslide volume as cumulative frequency percentage using the landslide event of November 2006 and the percentage values are expressed as probability. The probability that a landslide exceeds a volume of 1000 m³ and 10,000 m³ is estimated as 0.07 and 0.01, respectively. We will use these probability values as the components for estimation of the landslide hazard.

We have selected only two volume categories for landslides because of the fact that casualties and property losses (e.g., buildings or land use) are generally caused by landslides with relatively large failure volumes.

6. Temporal probabilities of landslides

The proposed model for quantitative landslide hazard requires an estimate of the temporal probability of landslides. The temporal probability was estimated indirectly using the exceedance probability of a rainfall threshold required to trigger landslides for the first time on natural slopes. The threshold is the minimum amount of rainfall needed to trigger landslides.

The availability of daily rainfall records and dates of landslide events allowed establishing threshold values for landslides on natural slopes. Daily rainfall data were collected from 13 rain gauges belonging to tea estates, the horticulture department and the railway office. The distribution of the rain gauges is shown in Fig. 1. All gauges are of the non-automated tipping bucket type, with daily recording of the readings in the morning.

Five events that occurred during the period between 1992 and 2006 in the months from October to December were used to manually draw an envelope curve adopting the method given in Jaiswal and van Westen (2009). For the threshold analysis, we used a 5-day antecedent rainfall (R_{5ad}) for establishing the threshold. The 5-day antecedent rainfall was found optimal for triggering landslides in the study area (Jaiswal and van Westen, 2009). The threshold line is represented by a linear mathematical equation ($R_T = 210 - 0.54 R_{5ad}$). The small slope (0.54) and high intercept (210) of the envelope curve indicate that such events either require very high magnitude daily rainfall or a very high amount of a five-day antecedent rainfall during the monsoon to trigger landslides.

The temporal probability of threshold exceedance on natural slopes, which also gives the probability of a landslide initiation $\{L\}$, for different time periods is estimated in four different parts of the areas as shown in Fig. 3 using the following probability model:

$$P\{(R > R_T) \cap L\} = P\{R > R_T\}P\{L | R > R_T\} \tag{3}$$

where R_T is the threshold value of rainfall (R). The probability model, Eq. (3), suggests that the probability of occurrence of both a rainfall that exceeds the threshold $\{R > R_T\}$ and landslides $\{L\}$ is equal to the probability of $\{R > R_T\}$ multiplied by the probability of occurrence of $\{L\}$, assuming that $\{R > R_T\}$ has already occurred. The probability of $\{R > R_T\}$ can be obtained by determining the exceedance probability of the rainfall threshold using a Poisson model and the probability of

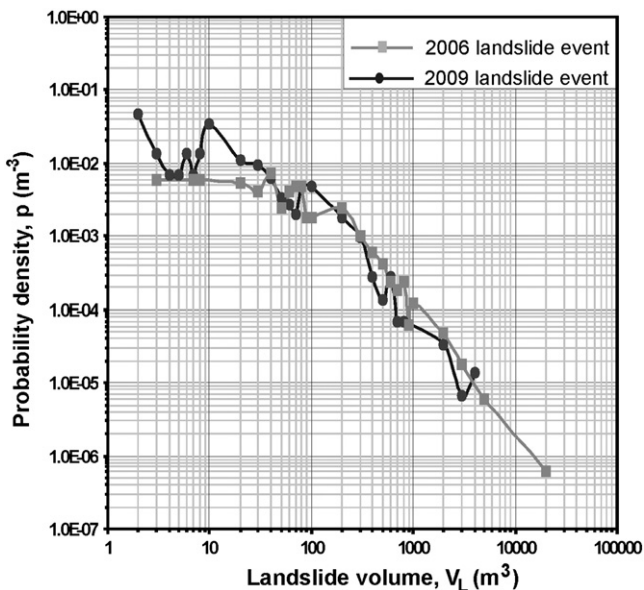


Fig. 6. Probability density distribution of landslide volume of 2006 and 2009 events.

$\{L R > R_T\}$ relies on the frequency of occurrence of landslides after the threshold has been exceeded.

For each section, based on the past rate of $R > R_T$, we obtained threshold recurrence i.e., the expected time between successive threshold exceedances. Knowing the mean recurrence interval of threshold in each section (from 1992 to 2006), and adopting a Poisson probability model, we computed the probability of the threshold being exceeded [$P\{R > R_T\}$] in different years (i.e., 1, 3, 5, 15, 25 and 50 years) in each section. Due to the possible incompleteness of the landslide data, we have taken the value of $\{L R > R_T\}$ in Eq. (3) as 0.73, which is the same as the one estimated for the entire railway route having the similar threshold equation (Jaiswal and van Westen, 2009). Since events triggering landslides on natural slopes require very high daily and antecedent rainfall, we assume that under the given high rainfall condition the likelihood of triggering landslides is also high, such as those estimated for the entire railway route. Using Eq. (3) we finally estimated temporal probability of landslide events for different time periods.

Table 1 shows the temporal probability in the four sections for different time periods, from 1 to 50 years. The results indicate that Sections I and III, and Sections II and IV have the same mean recurrence interval of the threshold and thus the temporal probability is also similar. The probability of one or more landslide events to occur in one to 50 years time varies from 0.13 to 0.73 in different sections. Sections I and III show a relatively high temporal probability of exceedance and they also have maximum incidences of recorded landslides. After 25 years all sections will have the maximum probability of exceedance of rainfall threshold [$P\{R > R_T\} = 1$] and thus have the highest probability of experiencing one or more landslide events (0.73).

7. Spatial probabilities of landslides

The spatial probability of landslides can be estimated using a variety of statistical techniques. Some of the commonly used techniques include logistic regression analysis (e.g., Atkinson and Massari, 1998; Ohlmacher and Davis, 2003; Suzen and Doyuran, 2004; Nefeslioglu et al., 2008), discriminant analysis (e.g., Baeza and Corominas, 2001; Carrara et al., 2003; Guzzetti et al., 2005), conditional analysis (e.g., Clerici et al., 2002), and weight of evidence (e.g., van Westen et al., 2003; Neuhauser and Terhorst, 2007). The above statistical techniques are usually based on two assumptions: first, that areas which have experienced landslides in the past are likely to experience them in the future and secondly, that areas with a similar set of geo-environmental conditions as that of the failed areas are also likely to fail in the future (Guzzetti et al., 1999; Fell et al., 2008). This means that the quantitative estimates of the spatial location of future landslide sources depend on the detailed information on the distribution of past landslides and a set of thematic variables such as slope angle, aspect, lithology, etc. that has initiated these landslides. The second assumption facilitates in predicting the geographical location of future landslides in passive areas (i.e., areas presently devoid of landslides) provided the geo-environmental

conditions remain the same. The above assumptions have been successfully used for statistically quantifying landslide susceptibility at a basin scale.

7.1. Selection and classification of preparatory factors

For susceptibility mapping, the selection of preparatory factors depends on the scale of analysis, the characteristics of the study area, the landslide type, the failure mechanisms and the priori knowledge of the main causes of landslides (Guzzetti et al., 1999; Glade and Crozier, 2005). It is essential to select those factors that bear a clear physical relationship with mass movement in the study area, otherwise the statistical analysis produce results that may be unreliable (Guzzetti et al., 1999). A systematic overview of the important preparatory factors required for susceptibility mapping in different scales is given in van Westen et al. (2008).

For the susceptibility mapping, we selected preparatory factors based on field observations, the characteristics of the mass movements and the landslide causative factors reported in the earlier studies of landslide susceptibility in the Nilgiri Hills. In the research area, landslides are individually small in size initiating as a debris slide and affect only the overburden soils and regolith. Failures are common in areas where slopes are steep and contain thick regolith cover (Figure 4A–C). From the field observations it is evident that slope angle, landuse type and thickness of regolith are the key factors that control mass movements in the area. Earlier reports on landslides, including studies on the landslide analysis where about 300 landslides triggered in 1978 and 1979 were investigated, have indicated slope angle, changes in the land use and thickness of regolith as the main causative factors for the initiation of debris slides and debris flow slides in the Nilgiri Hills (Seshagiri and Badrinarayanan, 1982). The report did not include lithology and structure as preparatory factors because they were observed to have no direct influence in causing landslides except in the development of overburden soils.

Based on the facts given in the earlier reports (Seshagiri and Badrinarayanan, 1982) and the present condition of mass movements, we selected four preparatory factors for the susceptibility modeling and classified them into 37 factor classes, used as independent variables: slope angle (13 classes), aspect (12 classes), land use (8 classes) and regolith thickness (4 classes). The dependent variable includes source areas of the existing landslides on natural slopes that occurred between 1987 and 2007 (Figure 3). A brief description of the significance and mapping techniques for each factor is given below.

- Slope angle – the slope gradient greatly influences the susceptibility of a slope to landsliding. In general landslide frequency increases with the slope gradient until the maximum frequency is reached in the 35–40° categories, followed by a decrease (Lee and Min, 2001; Dai and Lee, 2002). The high frequency of failures with increasing slopes may be attributed to reduce the shear strength in the overburden mass. For the study area, the slope angle was derived from a digitized topographic map with 10 m contour spacing that was interpolated in a 10 m regular grid DTM using Arc GIS 9.3. The slope map was reclassified into 13 classes with intervals of 5°. The landslide distribution indicates that landslide frequency increases with the slope angle until the maximum is reached in the 25°–30° categories, followed by a decrease. About 80% of the landslides are distributed between slope categories 15° to 40°. The areas with more vertical slopes with outcropping bedrock were found to be stable and not susceptible to landslides.
- Aspect – the aspect (direction) of a slope may also contribute to landsliding. The moisture retention and vegetation are generally reflected by the slope aspect, which may affect soil strength and susceptibility to landslides. The slope aspect was also derived from the DTM using Arc GIS 9.3 and the values were grouped into 12

Table 1
Temporal probability of landslide events (threshold equation: $R_T = 210 - 0.54 R_{5ad}$).

Area	Sections	$R > R_T^a$	Temporal probability for different periods (in years)					
			1	3	5	15	25	50
East of Burliyar	I	11	0.37	0.65	0.71	0.73	0.73	0.73
Around Hillgrove	II	3	0.13	0.33	0.46	0.69	0.73	0.73
Around Marapallam	III	11	0.37	0.65	0.71	0.73	0.73	0.73
West of Runnymede	IV	3	0.13	0.33	0.46	0.69	0.73	0.73

^a R_T is the threshold value of rainfall R .

classes with intervals of 30°. The correlation of landslides and aspect shows high failure percentages (>85%) between N120° and N210°, which could be because most part of the study area lies on the southern topographic slope of the Tiger Hill–Kori Betta Ridge.

- Land use – land use is the other important causative factor that can influence landslides. Changes in the land use pattern such as deforestation, or increase in the agricultural and constructional activities make an area more susceptible to landslides. During 1978 and 1979 most of the landslides (68.5%) occurred in the planted area (tea and coffee) and only 16% within the forested areas (Seshagiri and Badrinarayanan, 1982). In the study area, most of the steeper slopes are under the forest and gentler slopes are used for tea plantation. In the past 100 years not many changes in land use have taken place in the area except near Katteri where several new buildings have been constructed. The total area of the reserved forest and tea estates has not been changed over time. The land use map for the corridor area was prepared from the 1998 surveyed 1:25,000 scale topomap and Cartosat-1 stereo data (2.5 m resolution) of April 2007. Eight classes were obtained for the overlay of preparatory factors i.e., forest, scrubs, tea plantation, tea mixed with trees, coffee plantation, horticulture, barren areas and settlement. The forest covers about 13 km² (~60%) of the study area and its correlation with landslides shows high failure percentages (>85%).
- Regolith thickness – the thickness of regolith is another important preparatory factor for shallow landslides. In shallow landslides, where the slip plane is the contact zone of rock and regolith, a thin regolith cover increases the chance of landsliding due to the build-up of pore pressure on the contact (Iverson, 2000; Zezere et al., 2005). In the study area, a variation in the thickness of regolith was observed to be very erratic. On the hill slopes the thickness was found to vary significantly except near the Katteri area. The thickness depends on a large variety of factors, one important being the local variation in terrain morphology and therefore it is extremely difficult to predict the regolith thickness over the large areas. Ideally for thickness modeling a large number of observations (such as drill holes, outcrops, or geophysical measurements) are required. However, at a catchment scale this approach is difficult to implement. Given the above mentioned limitations and difficulties we used a point interpolation technique using the inverse distance weighing method to obtain a regolith thickness map for the study area. In a small catchment area of the Western Ghat of southern India interpolation methods have been used successfully for predicting soil depth (Kuriakose et al., 2009b). For interpolation, the points were measured at 246 locations in the field as the thickness of regolith cover exposed along the road, railroad, streams and landslide scars. The selected point locations were distributed in most parts of the study area, except towards the north where the slopes are very gentle and covered by tea plantations. Using the geostatistical software 'R', the measured points were then used to build up an empirical variogram, which was subjected to automatic fitting using a spherical model. The resulting partial sill was 14.2 and nugget of 13.1 with the maximum range of 573.3. These values were used in the interpolation at 10 m interval and a regolith thickness map was generated for the entire corridor area. The map was classified into four classes (i.e., 0 m, 1–5 m, 5–10 m and >10 m). The prediction of regolith thickness was better around areas where data were taken and the accuracy was lower in areas located away from the sample points. Since the density of sample points was high and closely located in areas that are susceptible to landslides the prediction of the regolith thickness was relatively better in these areas.

7.2. Selection of mapping units and susceptibility model

After the selection of appropriate preparatory factors, the next step is the selection of a mapping unit, which is the most basic, yet

important, component of any GIS based susceptibility analysis. The commonly used units are grid cell (pixel) based, which is a regular area of equal size or slope, which partition the territory into hydrological regions bounded by the drainage and divide lines (Carrara et al., 1992).

In reality, landslide processes are highly controlled by the slope features of the terrain, namely drainage and divide lines (Carrara et al., 1992) and therefore the slope units are best suited for hazard analysis. But for selecting a mapping unit importance must be given to the type of landslides in the area, mapping scale and scope of the work. In this study, the area of individual landslide sources is small and slope units covering relatively large surface area often do not match with the local geo-environmental setting bearing on slope instability. It is, therefore, taking any mapping unit of a size much larger than the landslide itself will result in an exaggeration of the area of actual landslide hazard. One way to overcome this is to resize the slope units according to the present landslide size by partitioning a river basin into nested subdivisions, coarser for larger landslides and finer for smaller failures (Guzzetti et al., 1999). But, for application purposes this approach is not suitable for small and shallow landslides (Montgomery and Dietrich, 1994). Furthermore, even with GIS it is still difficult to manually digitize irregular mapping units of a very small size e.g., the slope unit of area <100 m². In this work, because of the small size of the landslide source area, we selected pixels as the basic mapping unit for the susceptibility modeling so that the smallest landslide can be represented by a single pixel. As an additional advantage, a pixel-based mapping unit can facilitate very fast computation and processing of the raster data set in GIS. The 22 km² study area was converted into an equal-area grid by rasterizing the polygon map using a 10 m × 10 m pixel size.

For the susceptibility analysis, we used a logistic regression (LR) model in 'R-software' for the classification of spatial probability. The model helps in establishing a multivariate relation between a dependent (landslide) and several independent variables, which are the preparatory factors for landslides. In the LR model, the dependent variable z is dichotomous, which is a binary value and it is TRUE if a landslide is present and FALSE if it is absent, and independent variables are either categorical or continuous. The model aims to establish the probability that a mapping unit contains a landslide ($z = \text{TRUE}$) given the set of independent variables (Atkinson and Massari, 1998). The coefficients in the LR model are estimated using the maximum-likelihood method or in other words, the coefficients that make the observed results most 'likely' are selected. In the R-software, the regression model is fitted using iteratively reweighted least squares method under the link function (link = logit). The model uses Akaike's information criterion (AIC) to know the 'goodness' of the model in response to added independent variables or to know whether the model has gained anything by adding a variable (Venables et al., 2007).

7.3. Estimation of spatial probability

The logistic regression analysis is well known to have been designed to work on the dataset that are more or less equal in size (Garcia-Ruiz et al., 2003; Nefeslioglu et al., 2008) but there are many studies where the ratio of landslide presence (1)/landslide absence (0) is taken as unequal proportions (e.g., Atkinson and Massari, 1998; Guzzetti et al., 1999; Dai and Lee, 2002; Ohlmacher and Davis, 2003; Ayalew and Yamagishi, 2005). Studies have shown that where landslides are rare events i.e., if the mapping units with landslide presence are thousands of times fewer than their absence (King and Zeng, 2001), then taking unequal proportions of the ratio of landslide presence/absence the model tends to sharply under predict the probability of rare events (Garcia-Ruiz et al., 2003). Since, the susceptibility map produced by a logistic regression technique is directly controlled by the ratio of presence/absence of landslides in

the mapping units, any increase of mapping units free from landslides tends to decrease the areas susceptible to landslides in the susceptibility map. Contrary to this, the susceptible areas to landslides increase with a decrease in the ratio of absence/presence of landslides (Can et al., 2005). In this case study, the input dependent variable (landslide source area) is also a rare event as it is represented by 646 pixels, which is thousands of times fewer than their absence.

Can et al. (2005) recommended the use of an equal proportion of landslide presence/landslide absence if the event is considered rare. His recommendation was based on the study performing a series of sensitivity analyses using randomly selected different ratios of the mapping units with the absence of landslides to the mapping units including landslides. Following the above recommendation and the fact that landslides are rare events, we selected an equal number of pixels from the non landslide areas as samples representing the absence of landslide against the 646 pixels representing the presence of landslides. In this work we have used only one training dataset because studies have shown that selecting different training sets, randomly chosen from the landslide free areas, do not have much effect on the performance of the model (Yesilnacar and Topal, 2005).

The preparatory factors (slope angle, aspect, land use and regolith thickness) and landslide maps formed the input parameters for the susceptibility modeling. All factor maps were converted into an equal-area grid by rasterizing them using a 10 m × 10 m pixel size. The model was subjected to iterative modeling and at the initiation all the 37 factor classes (independent variables) were used. The model performed best under the given 37 variables and showed the lowest estimated AIC value (1255).

Judgment of the performance of the training dataset was based on the Receiver Operating Characteristics (ROC) curve (Zweig and Campbell, 1993). The ROC curve is a plot of the sensitivity (proportion of true positives) of the model prediction against the complement of its specificity (proportion of false positives), at a series of thresholds for a positive outcome. Sensitivity is the probability that a mapping unit with landslide is correctly classified, and is plotted on the y-axis in an ROC curve; sensitivity is the false negative rate. Specificity is the probability that a mapping unit with no-landslide is correctly classified; 1 – specificity is the false positive rate and is taken along the x-axis of the curve. The area under the curve represents the probability that the landslide susceptibility value for a landslide mapping unit calculated by the model will exceed the result for a randomly chosen no-landslide mapping unit. The ROC curve for the model developed is given in Fig. 7 and the area under the curve obtained is 0.856, which gives an accuracy of ~86% for the training model.

Table 2 shows the coefficients of different factor classes derived from the logistic regression model. The positive and negative coefficients respectively indicate the contribution of the variable towards increasing and reducing the likelihood of landslides in the mapping unit. As an example, almost all classes of slope and regolith thickness, southerly facing slopes (aspect ~151°–180°), forest and scrubs favour the probability of the occurrence of landslides. To the contrary, NE and SW facing slopes in a mapping unit are in favour of its stability. The estimated coefficients from the model output were used to compute the spatial probability value at each pixel.

Although the pixel-based mapping unit facilitated easier and faster computations of the susceptibility in GIS, however in reality a pixel doesn't represent morphological changes in the ground. Landslide processes, including the extent of source area and run-out of debris flow are highly controlled by the slope features of the terrain (Carrara et al., 1992). In fact, it is relatively easy to visualise and interpret maps in the field if the results are shown within a slope feature bounded by drainages and divide lines. This also helps to use the susceptibility map for all practical purposes, including the integration of landslide size larger than the size of a pixel. For this reason, we partitioned the study area into 2234 slope units, which were identified and digitized

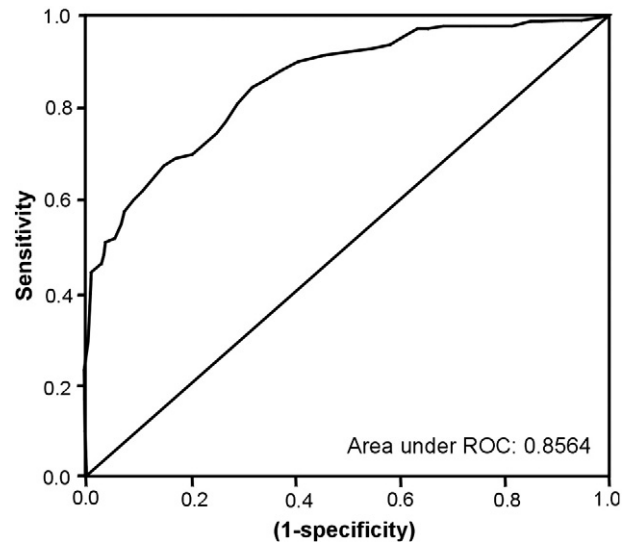


Fig. 7. Receiver operator characteristic curve.

manually from the topographic map. Each slope unit contains an area bounded by drainage lines, ridge line or breaks in slope. The average area of a slope unit is about 9848 m², corresponding to about 99 pixels of 10 m × 10 m. For each slope unit, we assigned a single susceptibility (probability) value taken from the maximum distributed spatial probability values of pixels within the slope unit.

Fig. 8 shows the spatial probability map after up-scaling the pixel-based mapping unit to the slope facet-based mapping unit. The susceptibility is expressed in terms of the estimated spatial probability of a landslide occurring in a slope unit under the given geo-environmental conditions. About 20% of the unit areas (4.3 km²) has

Table 2
Coefficients derived from logistic regression model.

Description of factor class	Class code	Coefficient
Intercept		– 5.7784
Slope		
05°–10°	SLOPEB	1.2570
10°–15°	SLOPEC	1.7167
15°–20°	SLOPED	2.9539
20°–25°	SLOPEE	2.5274
25°–30°	SLOPEF	2.6558
30°–35°	SLOPEG	3.1236
35°–40°	SLOPEH	3.5827
40°–45°	SLOPEI	2.2458
45°–50°	SLOPEJ	2.6026
50°–55°	SLOPEK	4.2675
55°–60°	SLOPEL	18.100
>60°	SLOPEM	– 13.376
Aspect		
31°–60°	ASPB	– 0.6701
61°–90°	ASPC	– 2.8454
91°–120°	ASPD	– 2.4312
121°–150°	ASPE	– 0.2060
151°–180°	ASPF	0.2995
181°–210°	ASPG	– 0.5400
211°–240°	ASPH	– 0.4798
241°–270°	ASPI	– 0.8326
271°–300°	ASPJ	– 18.391
Land use		
Forest	LANDB	1.8341
Settlement	LANDC	1.6921
Barren	LANDD	– 4.4342
Coffee	LANDE	– 15.348
Horticulture	LANDF	4.1669
Scrubs	LANDG	1.5271
Tea with trees	LANDH	– 16.300
Regolith thickness		
1–5 m	REGTHB	1.2169
5–10 m	REGTHC	2.1330
10–20 m	REGTHD	2.3162
AIC		1255

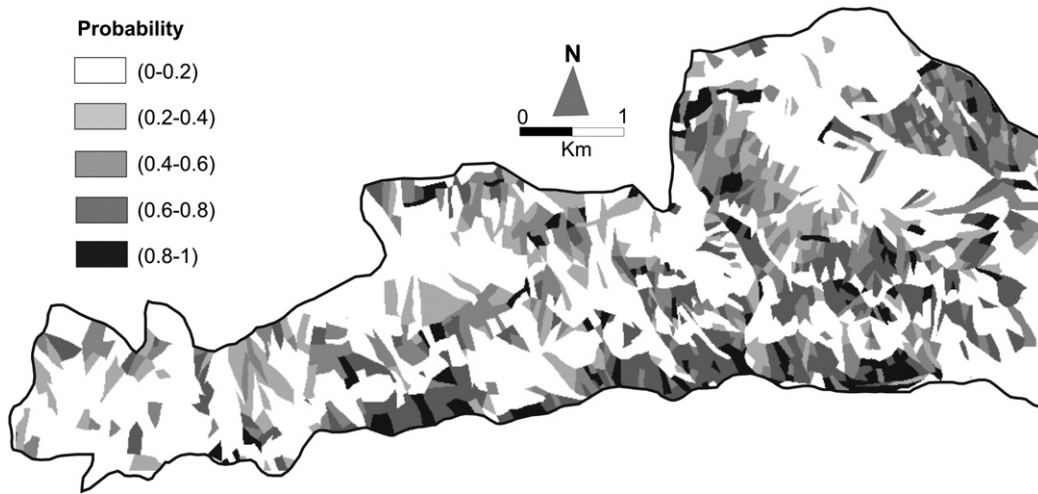


Fig. 8. Landslide susceptibility map of the study area.

an estimated probability of more than 0.6 and can be viewed as highly susceptible to landslides.

The statistical method was able to classify the study area into different susceptibility classes but the question remains how well the model has performed in classifying the area? The quantitative estimate of its performance was evaluated by using reliability tests, such as error matrix and success rate curve.

The error matrix is a straightforward way of testing a model fit by computing the percentage of cases (i.e., percentage of mapping units) correctly classified by the susceptibility model. It requires a base map containing known cases having known stable and unstable slopes. The most commonly used cases are known landslides from the inventory (Guzzetti et al., 2006), and a mapping unit is considered stable if it is free of landslide and unstable if it contains a landslide. For the susceptibility model, the mapping units are considered unstable if the units have a probability value >0.6 and stable if the probability is ≤0.6.

Table 3 shows the results of the error matrix for the logistic regression model shown in Fig. 8. The error matrix figures represent a measure of the “overall goodness of fit” of the susceptibility model (Guzzetti et al., 2006). The model has correctly classified about 74% of the mapping units in either stable or unstable group. It has also correctly classified about 70% of the unstable areas but misclassified about 30% of the landslide units to the stable group. About 26% of the mapping units that are now free of landslides were classified as “unstable” by the model. These are the areas that have environmental conditions typical of unstable slopes and could be the source of future landslides.

The error matrix provides the estimate for model fit or “overall goodness of fit” but does not provide a detailed description of the model performance of the different susceptibility classes. The model performance was judged using a success rate curve proposed by Chung and Fabbri (1999). The success rate curve was obtained using landslides that

Table 3
Comparison between mapping units classified as stable or unstable by the LR model and mapping units free of and containing landslides in the inventory map.

		Predicted groups (model)	
		Stable group	Unstable group
Actual Groups (inventory)	Stable mapping units free of landslides in the inventory	74%	26%
	Unstable mapping units containing of landslides in the inventory	30%	70%

Overall percentage of mapping units correctly classified = 74%.

were previously used in building the model. It was calculated by ordering the pixels of a susceptibility map in a number of classes, from high to low values. The success rate indicates how much percentage of all landslides occurs in the classes with the highest susceptibility values. It measures the effectiveness of the model and is a useful indicator for the quality of the map (van Westen et al., 2003).

The success rate curve (Figure 9) shows that 80% of all landslide sources are predicted by 35% of the classes with the highest value in the susceptibility map. Most of the landslides shown in the inventory map are in areas classified as susceptible by the model, and only 10% of the slope failures are in areas classified as not or weakly susceptible (probability ≤0.40) by the model.

8. Landslide hazard assessment

After estimating the magnitude probability of landslide volume (P_M), the temporal probability (P_T) of rainfall triggering landslide

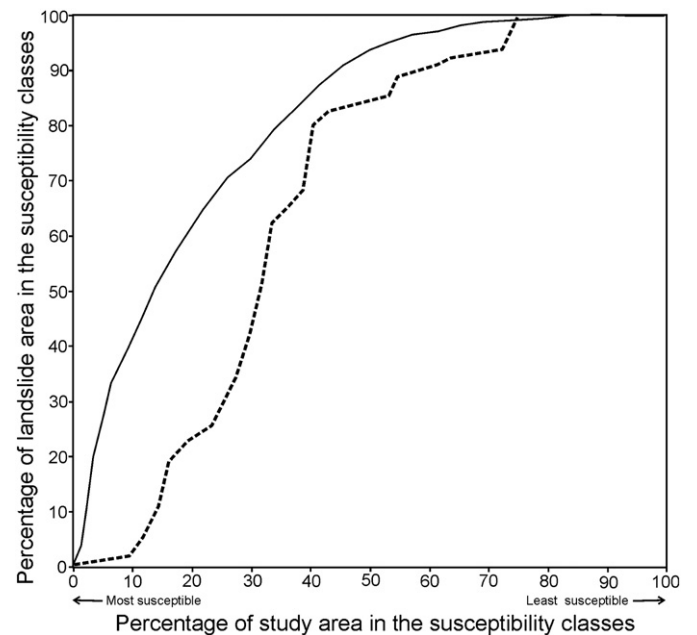


Fig. 9. Continuous thin line shows success rate curve (model fit). The x-axis of the graph shows the percentage of map with highest probability values and y-axis shows the percentage of debris slide area in each susceptible classes. Dashed line shows model prediction skills based on November 2009 landslide events.

events (Table 1), and the spatial probability (P_s) of landslides through logistic regression analysis (Figure 8), they were combined by estimating the joint probability using Eq. (1).

Fig. 10 shows examples of the obtained landslide hazard assessment. The Figure portrays landslide hazard for slope units in the north of Marapallam for six periods (1, 3, 5, 15, 25 and 50 years), and for two landslide volumes (larger than 1000 m^3 and $10,000 \text{ m}^3$). The joint probability in the Fig. 10 indicates that a slope unit will be affected by future landslides that exceed a given volume, in a given

time, and due to the local environmental setting. A total of 12 landslide hazard maps were generated each representing a specific scenario i.e., a specific time period and a landslide size.

9. Validation of models

All models used in the hazard analysis need to be validated for their performance in forecasting landslides (Chung and Fabbri, 2003; Fell et al., 2008). Validation can best be performed using landslides

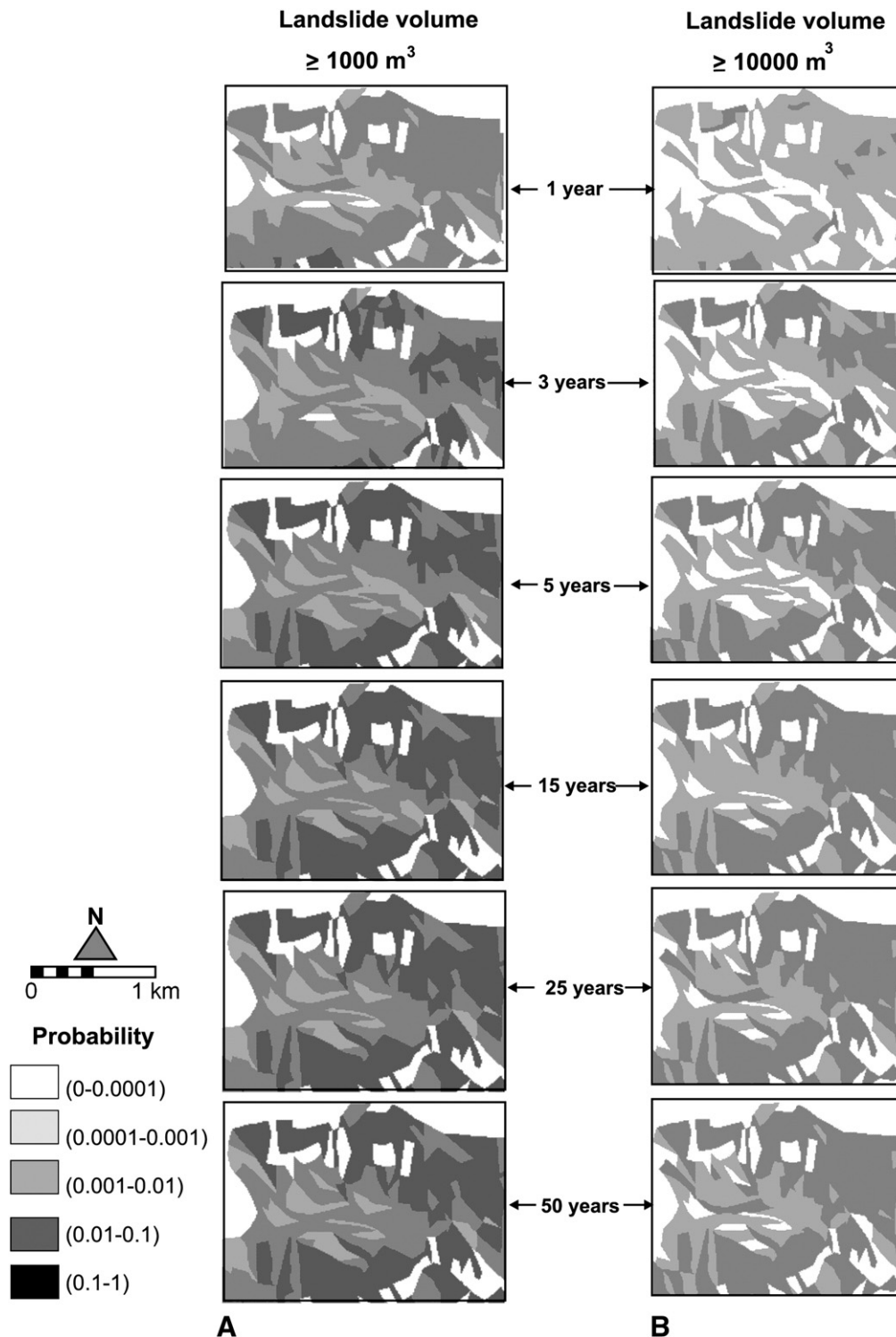


Fig. 10. Examples of landslide hazard maps for 6 periods, from 1 to 50 years, and for two landslide volumes, $V_L \geq 1000 \text{ m}^3$ (A) and $V_L \geq 10,000 \text{ m}^3$ (B). The probability gives the joint probabilities of landslide volume, of landslide temporal occurrence, and of landslide spatial occurrence.

independent from the one used to obtain the susceptibility map (Chung et al., 1995). The availability of information on landslide events of November 2009 provided us an opportunity to validate the models used in the assessment of landslide hazard in this case study.

A landslide inventory was prepared from the railway slip register and landslide technical reports. Field mapping was carried out in February 2010 to spatially map the recorded landslides. A total of 147 landslides were identified and mapped. The size (volume) of landslides ranges from 2 to 3600 m³. Landslides are mostly debris slides and debris flow slides that occurred on both cut slopes (136 slides) and on the natural slopes (11 slides). On cut slopes landslides are mostly reactivated old slides and on natural slopes they occurred as the first-time failures. Fig. 11 shows the spatial distribution of landslides on natural slopes. Most landslides triggered around Katteri and Marappalam area due to a very high rainfall that occurred between 8 and 10 November 2009. The three days cumulative rainfall was recorded the highest in the Coonoor area (937 mm) and lowest in the Kallar farm (202 mm). At some places torrent streams have resulted in the overbank failures and debris flows.

9.1. Validation of a rainfall threshold model

For the validation of the threshold model we have followed the method given in Jaiswal and van Westen (2009). Each rise in the threshold curve indicates that either there is a sudden increase in the magnitude of daily rainfall or there is a constant rise in five days antecedent rainfall. The crossover of the threshold curve from negative to positive values is taken as an indication of the conditions favourable for landsliding. One or more landslide events are expected before the positive curve decays to the zero threshold value.

Fig. 12 shows the performance of the threshold model ($R_T = 210 - 0.54 R_{5ad}$) for natural slopes during October to December 2009. In Burliyar area, landslides occurred on 10 November when the rainfall crosses the threshold value, whereas in Hillgrove and in Runneymede landslides occurred on both 8 and 9 November when the threshold was high. In the Kallar area, rainfall did not cross the threshold value and therefore no landslide occurred in this part of the study area (Figure 11). Similarly in 2008, the threshold did not exceed in any of the rain gauges and no landslide occurred in the study area.

The threshold model has performed well and accurately forecasted landslide events in 2009. The probability of a landslide event to occur given the threshold exceedance $P[L R > R_T]$ is equal to 1 during 2008 and 2009, which indicates that the threshold model is capable of accurately forecasting landslides on natural slopes.

The probability of occurrence of one or more landslide events in a 3 year time period was estimated high (~0.65) in Sections I and III and relatively low (~0.33) in Sections II and IV (Table 1). However, in 2009 rainfall triggered landslides in all sections, except in Section I. An amount of rainfall similar to the 2009 events has never been recorded during the period of analysis (1987 to 2007). Such a high rainfall is actually a rare event in the study area. In the recent past, a very high rainfall occurred in 1979 that resulted in floods and landslides around the Coonoor area (Seshagiri and Badrinarayan, 1982).

9.2. Validation of probability of landslide size

For the validation of the probability of the landslide size, we obtained the probability density distribution of the landslide volume of 147 landslides of the 2009 event and compared the result with that of the 2006 event. Fig. 6 shows the probability density distributions of both 2006 and 2009 events. In 2009, the distribution shows distinct roll-over for failure volumes of less than 10 m³ whereas 2006 event shows flattening of the curve instead of a distinct roll-over for failure volumes of less than 200 m³. However, in both the distribution the linear portion of the curve (volume >200 m³ in 2006 and volume >80 m³ in 2009) shows a power relationship with power law scaling exponent as -1.7 . In 2009 the probability of landslides exceeding 1000 m³ is 0.04, which is smaller than 2006. In fact in 2009 small landslides (volume <100 m³) occurred in relatively large numbers in comparison to 2006, because of the fact that most landslides in 2009 triggered within Sections III and IV (see Figure 3 for the section boundaries), where slopes are relatively gentle and covered by tea plantation.

9.3. Validation of landslide susceptibility model

For the analysis of the prediction rate we have used the model proposed by Chung and Fabbri (2003). We computed the proportion of the landslide area of 2009 events in each susceptibility class, and showed the results using cumulative statistics. Fig. 9 shows the percentage of the study area, ranked from most to least susceptible (x-axis), against the cumulative percentage of the area of the triggered landslides in each susceptibility class (y-axis), represented by a dashed black line.

The prediction rate curve (Figure 9) shows that the most susceptible 20% of the study area contains 22.3% of the landslide source area. This 20% of the susceptible areas also contain slopes that are located east of the study area, where most of the high susceptible slopes are located. The model was able to predict about 35% of the

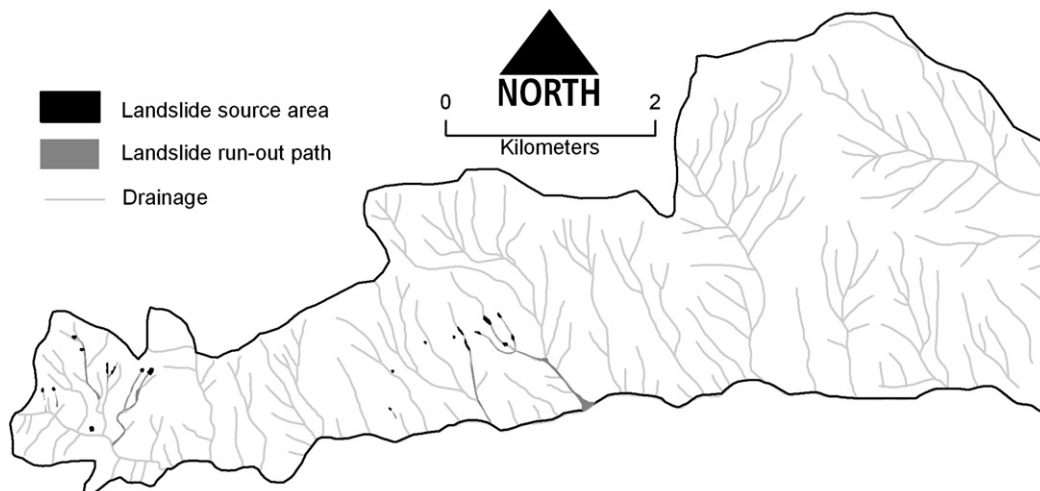


Fig. 11. Spatial distribution of landslides on natural slopes triggered in 2009.

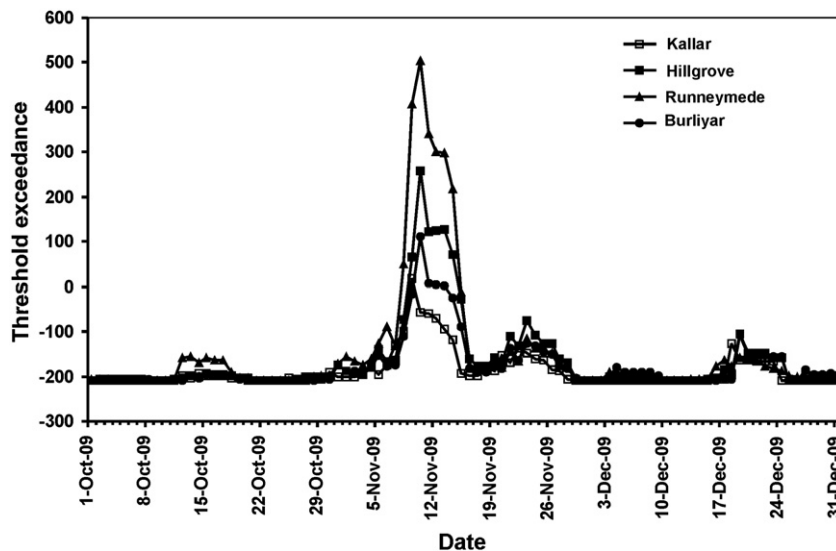


Fig. 12. Validation of the threshold equation ($R_T = 210 - 0.54 R_{5ad}$) for natural slopes. Positive values on the y-axis indicate threshold exceedance ($R > R_T$).

landslide areas as unstable group (spatial probability ≥ 0.6). Further, the most susceptible 33% (spatial probability > 0.4) of the study area contains 65% of the landslide areas whilst 80% of the landslide areas are predicted by the most susceptible 40% of the study area. Most of the landslides shown in the inventory map (Figure 11) are in areas classified as susceptible by the model, and 16% of the slope failures are in areas classified as low susceptible (probability ≤ 0.20) by the model. The prediction of the model is low in high susceptible areas, which is because of the fact that most landslides in 2009 occurred around Katteri (western part of the study area), where slopes are having a relatively low probability value. It is reasonable to accept that if a landslide event triggers landslides in the eastern part of the study area then the prediction rate could be much better.

The result shown in Fig. 9 provides a quantitative estimate of the model prediction skill. As observed by others researchers (e.g. Chung and Fabbri, 2003; Guzzetti et al., 2005) the prediction rate of a susceptibility model is often lower than the success rate of the model. In this validation test the prediction of the susceptibility model is also slightly lower than the model fitting performance shown in Fig. 9 (continuous thin line).

10. Discussion and conclusions

Landslide hazard identification is often carried out with an aim to scope the nature of the potential threat but it is equally useful to carry out the hazard analysis independent of existing human constructs as shown in this study. In later case, the obtained hazard can be used as a powerful guide to future development decisions (Crozier and Glade, 2005). With the availability of information on 'where' and 'when' a landslide is expected, expressed in terms of probabilities, land use planning for future development for a specified time period, say 10 years or 50 years can be made.

The proposed method allowed us to determine quantitative hazard of first-time slope failures in a data scarce inventory. Since the inventory is incomplete and the landslides are small and non-repetitive (occurring as first-time failures) therefore the traditional method of computing the frequency of slope failures based on the recurrence of landslides was not applicable in this case. Rather the historical records, with the availability of information on rainfall and the date of occurrence of landslides, made the estimation of the (temporal) probability of occurrence of landslides and the calculation of hazard feasible, which was otherwise difficult.

The susceptibility model used to predict the spatial probability of potential landslides is based on certain assumptions. It is assumed

that landslides will occur in future under the same conditions and triggering factors that produced them in past. One has to take into account that geo-environmental conditions of an area such as land use or hydrological conditions may change due to human action. Conditions may also change when the source of a landslide is exhausted by earlier landsliding or the morphology of the slope is changed and becomes stable (Guzzetti et al., 2005). However, we would like to state that to some extent the assumption holds true for the study area. The preparatory factors (e.g., aspect, slope and regolith thickness) are not expected to change significantly in a short time period, say in a 50 year time. Local morphological changes may occur due to landsliding but this will not substantially affect the susceptibility model because most landslides on natural slopes are first-time failures. Also the land use has been rather static, and the total area of the reserved forest and tea estates, which cover about 90% of the area, have not changed for the past 100 years except for a limited human interference near the Katteri area.

For the susceptibility modeling, we considered only four landslide preparatory factors on the basis of field condition and the type of mass movements present in the area. This selection was also from the application point of view. In the Nilgiri area, if a building is to be constructed then it is mandatory to obtain permission from the Geo-technical office at Coonoor for landslide risk. Till now the office follows the earlier work of the Geological Survey of India (Seshagiri and Badrinarayanan, 1982) for evaluating landslide susceptibility. The official physically inspects the building site, which can be smaller than a pixel size used, and collects data on factors used in the model (e.g., slope, land use, etc.). The field data were then compared with the susceptibility rating in order to evaluate the susceptibility of the slope where the building is to be located. Given the working guidelines of the Geo-technical office, we were also asked to prepare a susceptibility model based on factors that can be easily measured in the field so that the model can be implemented for planning purposes. Therefore, we used limited factors for modeling susceptibility and nevertheless through validation we have showed that the model is capable of forecasting future slope failures.

The temporal probability of landslides was estimated indirectly from landslide events using the mean rate of occurrence of the threshold rainfall. In the Nilgiri area all landslides are rainfall induced and occur mostly during October to December due to the retreating monsoon. However, a very high rainfall occurring due to some local phenomena may affect the distribution of landslide events in the area, similar to one observed in 2009. The temporal probability gives the probability of occurrence of one or more landslide events in a

particular area in a given time period. As expected the probability increases with the increase in the length of the time period such that the maximum value (0.73) is reached for a 25 year period. In more than 25 years time it is always certain to have at least one landslide event. Here the highest probability is 0.73 and not 1 because in earlier studies (Jaiswal and van Westen, 2009) we have shown that all rainfall exceeding threshold value do not trigger landslides rather the success is only 0.73 i.e., 73% of cases the rainfall triggers landslides if exceeded. Due to the possible gap in the record, we have taken 0.73 as the success of the threshold model for triggering landslides on the natural slopes.

For the threshold modeling we considered all landslide events irrespective of the number and sizes of landslides they triggered. The temporal model can be improved further if the threshold can be generated separately for different landslide sizes and landslide densities, but such an exercise requires a more detailed landslide and rainfall inventory, and for a long time period. Substantially complete event-based landslide inventories along with known dates of landslide events are seldom available particularly for past dates.

Guzzetti et al. (1999) proposed to include landslide magnitude, as a proxy for landslide destructiveness, in the hazard analysis to complete the definition of hazard given by Varnes (1984). Destructiveness or damage caused by a landslide largely depends on the volume of a displaced material, and the velocity and kinetic energy of the flow. For a catchment scale study these parameters are extremely difficult to obtain and to integrate in the hazard zoning. Information on landslide volume is difficult to obtain if inventory is prepared from remote sensing data, and therefore the landslide area is commonly used as a proxy for landslide magnitude (Guzzetti et al., 2005). In this study, the availability of data on volume from historical records has facilitated using volume as a proxy for landslide magnitude, which is the better measure of landslide destructiveness.

The assumption that the three probabilities i.e., the probabilities of landslide volume, the temporal probability of landslide event and the spatial probability of slope failures are independent is necessary to make the multiplication of the three probabilities statistically feasible. To some extent the assumption may hold true for this case study. The temporal probability is based on rainfall, which is the main trigger of landslides in the area. For the threshold analysis we have considered all landslide events irrespective of the number of landslides they triggered and the spatial distribution of landslides. Therefore, the threshold is not directly dependent on a particular terrain condition within the study area. Further for the susceptibility modeling we did not consider rainfall as a factor or landslides related to a specific rainfall event, rather we considered all landslides in the study area as a dependent variable. Therefore it is reasonable to accept that both spatial and temporal probabilities of landslides are independent.

In nature the number of landslides and the proportion of large to small landslide volume can vary according to the intensity of rainfall. It is expected that a very high intensity rainfall can trigger more number of landslides and of a larger volume than a rainfall of relatively low intensity. Thus, both rainfall and frequency-size distribution of landslide are mutually dependent. On contrary, in this case study it is observed that a very high rainfall event of 2009 has resulted in less number of landslides and of relatively smaller volumes than in 2006 (Figure 6). This difference is mainly because of the contrast in the terrain condition where most landslides have occurred in 2006 and 2009. Landslides in 2006 occurred in relatively steeper slopes than in 2009. Thus, we can say that the frequency-size distribution of landslides is not directly dependent on the rainfall condition, rather it is more related to the terrain type. However, in other studies, based on a handful of complete inventories, researchers (e.g., Guzzetti et al., 2002; Malamud et al., 2004) have demonstrated that the probability density of landslide size does not change significantly with changing physiographical conditions. Malamud et al. (2004) showed that the probability density distribution are

virtually identical for landslides triggered by three different triggers in three different physiographical regions (e.g., co-seismic landslides in southern California, rainfall induced landslides in Guatemala, Central America and landslides due to rapid snow melting in Umbria, Italy). For simplicity, like other studies we also assume that the probability distribution of the landslide size is independent of the terrain type.

In this study, we have noticed that a relatively high susceptible areas (e.g., east of Burliyar) can be of low hazard in a given time if the rainfall does not exceed the threshold value (e.g., 2009 event east of Burliyar) or vice versa. The hazard of an area is therefore conditionally dependent on the probability of occurrence of a landslide triggering rainfall event and the susceptibility of the terrain. Due to the difficulty in evaluating conditional probabilities its multiplication remains the best option to evaluate hazard. The model can be further improved when better ways of generating more accurate measures of the thematic variables and hazard model become available. One way to improve a hazard model is to incorporate event-based landslide inventories and make separate spatial probabilities, temporal and size probabilities per return period of the triggering event that caused the event-based landslides (e.g., Glade, 2001). But as a major drawback the multi-temporal event-based landslide inventories are seldom available.

The proposed hazards models are based on a limited landslide inventory. For example, the susceptibility model is based on landslides that are mostly located in the eastern part of the study area. When new information on spatial, temporal or size of landslides becomes available, the hazard models can be revised. The models can be used to estimate hazard for different time scenarios for the purpose to provide quantitative expertise on future slope failures to planners, disaster management authorities, decision makers and individual landowners. The models provide information on the likelihood of the initiation of future slope failures in an area and not the area that are likely to be inundated by debris. For the latter case run-out areas are needed to be incorporated in the hazard model. The availability of information on the 2009 landslide events has given us the opportunity to validate the models used in the hazard analysis. But still we have to “wait and watch” for more events to occur in order to validate the hazard map for different time scenarios.

Acknowledgements

We acknowledge the help of Southern Railway, Geo-technical Cell and Tea Estates of Coonoor, Tamilnadu, India for the relevant data and support. The research was carried out under the United Nations University–ITC School on Disaster Geo-Information Management (<http://www.itc.nl/unu/dgim>).

References

- Atkinson, P.M., Massari, R., 1998. A generalized linear modeling of susceptibility to landsliding in the Central Apennines, Italy. *Computers & Geosciences* 24 (4), 373–385.
- Ayalew, L., Yamagishi, H., 2005. The application of GIS-based logistic regression for landslide susceptibility mapping in the Kakuda–Yahiko Mountains, Central Japan. *Geomorphology* 65, 15–31.
- Baeza, C., Corominas, J., 2001. Assessment of shallow landslide susceptibility by means of multivariate statistical techniques. *Earth Surface Processes and Landforms* 26, 1251–1263.
- Balachandran, V., Thanavelu, C., Pitchaimuthu, R., 1996. Marappalam landslide, the Nilgiri district, Tamilnadu, India: a case study. *Proceedings of International Conference on Disasters and Mitigation, Madras, India. 9–22 January 1996*, I: A4–21–23.
- Brardinoni, F., Church, M., 2004. Representing the landslide magnitude–frequency relation: Capilano river basin, British Columbia. *Earth Surface Processes and Landforms* 29, 115–124.
- Can, T., Nefeslioglu, H.A., Gokceoglu, C., Sonmez, H., Duman, T.Y., 2005. Susceptibility assessments of shallow earthflows triggered by heavy rainfall at three catchments by logistic regression analyses. *Geomorphology* 72, 250–271.
- Carrara, A., Cardinali, M., Guzzetti, F., 1992. Uncertainty in assessing landslide hazard and risk. *ITC Journal* 2, 172–183.

- Carrara, A., Crosta, G.B., Frattini, P., 2003. Geomorphological and historical data in assessing landslide hazard. *Earth Surface Processes and Landforms* 28 (10), 1125–1142.
- Cascini, L., Bonnard, Ch., Corominas, J., Jibson, R., Montero-Olarte, J., 2005. Landslide hazard and risk zoning for urban planning and development. In: Hungr, O., Fell, R., Couture, R., Eberhardt, E. (Eds.), *Landslide Risk Management*. Taylor and Francis, London, pp. 199–235.
- Catani, F., Casagli, N., Ermini, L., Righini, G., Menduni, G., 2005. Landslide hazard and risk mapping at catchment scale in the Arno River basin. *Landslides* 2, 329–342.
- Chau, K.T., Sze, Y.L., Fung, M.K., Wong, W.Y., Fong, E.L., Chan, L.C.P., 2004. Landslide hazard analysis for Hong Kong using landslide inventory and GIS. *Computers & Geosciences* 30, 429–443.
- Chleborad, A.F., Baum, R.L., Godt, J.W., 2006. Rainfall thresholds for forecasting landslides in the Seattle, Washington, area — exceedance and probability. USGS Open-File Report 2006-1064. available at: <http://www.usgs.gov/pubprod>, cited on 15 July 2008.
- Chung, C.J., Fabbri, A.G., 1999. Probabilistic prediction models for landslide hazard mapping. *Photogrammetric Engineering and Remote Sensing* 65 (12), 1389–1399.
- Chung, C.F., Fabbri, A.G., 2003. Validation of spatial prediction models for landslide hazard mapping. *Natural Hazards* 30, 451–472.
- Chung, C.F., Fabbri, A.G., Van Westen, C.J., 1995. Multivariate regression analysis for landslide hazard zonation. In: Carrara, A., Guzzetti, F. (Eds.), *Geographic Information Systems in Assessing Natural Hazards*. Kluwer, Dordrecht, pp. 107–133.
- Clerici, A., Perego, S., Tellini, C., Vescovi, P., 2002. A procedure for landslide susceptibility zonation by the conditional analysis method. *Geomorphology* 48, 349–364.
- Coe, J.A., Michael, J.A., Crovelli, R.A., Savage, W.Z., 2000. Preliminary map showing landslide densities, mean recurrence intervals, and exceedance probabilities as determined from historic records, Seattle, Washington. USGS Open-File Report 00-0303. available at: <http://pubs.usgs.gov/of/2000/ofr-00-0303>, cited on 15 July 2008.
- Corominas, J., Moya, J., 2008. A review of assessing landslide frequency for hazard zoning purposes. *Engineering Geology* 102, 193–213.
- Crozier, M.J., 1999. Prediction of rainfall-triggered landslides: a test of the antecedent water status model. *Earth Surface Processes and Landforms* 24, 825–833.
- Crozier, M.J., Glade, T., 2005. Landslide hazard and risk: Issues, Concepts and Approach. In: Glade, T., Anderson, M., Crozier, M.J. (Eds.), *Landslide Hazard and Risk*. John Wiley and Sons Ltd, West Sussex, England, pp. 1–40.
- Dai, F.C., Lee, C.F., 2002. Landslide characteristics and slope instability modeling using GIS, Lantau Island, Hong Kong. *Geomorphology* 42, 213–228.
- Devoli, G., Morales, A., Hoeg, A., 2007. Historical landslides in Nicaragua — collection and analysis of data. *Landslides* 4 (1), 5–18.
- Fell, R., Corominas, J., Bonnard, C., Cascini, L., Leroi, E., Savage, W.Z., 2008. Guidelines for landslide susceptibility, hazard and risk zoning for land use planning. *Engineering Geology* 102, 85–98.
- García-Ruiz, J.M., Lorente-Grima, A., Begueria-Portugues, S., Marti-Bono, C., Valero-Garces, B., Lopez-Moreno, J.I., 2003. Damocles Project Report. Contract No EVG1-CT-1999-00007. Instituto Pirenaico de Ecología, CSIC, Zaragoza, Spain, p. 20.
- Glade, T., 2001. Landslide hazard assessment and historical landslide data — an inseparable couple? In: Glade, T., Albini, P., Frances, F. (Eds.), *The use of historical data in natural hazard assessments — advances of technological and natural hazard research*. Kluwer, Norwell, pp. 153–169.
- Glade, T., Crozier, M.J., 2005. A review of scale dependency in landslide hazard and risk analysis. In: Glade, T., Anderson, M., Crozier, M.J. (Eds.), *Landslide Hazard and Risk*. John Wiley and Sons Ltd, West Sussex, England, pp. 75–138.
- Guthrie, R.H., Evans, S.G., 2004. Magnitude and frequency of landslides triggered by a storm event, Loughborough Inlet, British Columbia. *Natural Hazards and Earth System Sciences* 4, 475–483.
- Guzzetti, F., Cardinali, M., Reichenbach, P., 1994. The AVI project: a bibliographical and archive inventory of landslides and floods in Italy. *Environmental Management* 18 (4), 623–633.
- Guzzetti, F., Carrara, A., Cardinali, M., Reichenbach, P., 1999. Landslide hazard evaluation: a review of current techniques and their application in a multi-scale study, Central Italy. *Geomorphology* 31, 181–216.
- Guzzetti, F., Malamud, B.D., Turcotte, D.L., Reichenbach, P., 2002. Power-law correlations of landslide areas in Central Italy. *Earth and Planetary Science Letters* 195, 169–183.
- Guzzetti, F., Reichenbach, P., Cardinali, M., Galli, M., Ardzizzone, F., 2005. Probabilistic landslide hazard assessment at the basin scale. *Geomorphology* 72, 272–299.
- Guzzetti, F., Reichenbach, P., Ardzizzone, F., Cardinali, M., Galli, M., 2006. Estimating the quality of landslide susceptibility models. *Geomorphology* 81, 166–184.
- Harp, E.L., Reid, M.E., McKenna, J.P., Michael, J.A., 2009. Mapping of hazard from rainfall-triggered landslides in developing countries: examples from Honduras and Micronesia. *Engineering Geology* 104, 295–311.
- Iverson, R.M., 2000. Landslide triggering by rain infiltration. *Water Resources Research* 36, 1897–1910.
- Jaiswal, P., van Westen, C.J., 2009. Estimating temporal probability for landslide initiation along transportation routes based on rainfall thresholds. *Geomorphology* 112, 96–105.
- King, G., Zeng, L., 2001. Logistic regression in rare events data. *Political Analysis* 9 (2), 137–163.
- Kuriakose, S.L., van Beek, L.P.H., van Westen, C.J., 2009a. Parameterizing a physically based shallow landslide model in a data poor region. *Earth Surface Processes and Landforms* 34 (6), 867–881.
- Kuriakose, S.L., Devkota, S., Rossiter, D.G., Jetten, V.G., 2009b. Prediction of soil depth using environmental variables in an anthropogenic landscape, a case study in the Western Ghats of Kerala, India. *Catena* 79, 27–38.
- Lee, S., Min, K., 2001. Statistical analysis of landslide susceptibility in Yongin, Korea. *Environmental Geology* 40, 1095–1113.
- Lee, S., Pradhan, B., 2006. Probabilistic landslide hazards and risk mapping on Penang Island, Malaysia. *Journal of Earth System Science* 115 (6), 661–672.
- Lips, E.W., Wiecek, G.F., 1990. Recurrence of debris flows on an alluvial fan in central Utah. In: French, R.H. (Ed.), *Hydraulic/Hydrology of Arid Lands*, Proc. of the Int. Symp. American Society of Civil Engineers, pp. 555–560.
- Malamud, B.D., Turcotte, D.L., Guzzetti, F., Reichenbach, P., 2004. Landslide inventories and their statistical properties. *Earth Surface Processes and Landforms* 29 (6), 687–711.
- Montgomery, D.R., Dietrich, W.E., 1994. A physically based model for the topographic control of shallow landsliding. *Water Resources Research* 30 (4), 1153–1171.
- Nefeslioglu, H.A., Gokceoglu, C., Sonmez, H., 2008. An assessment on the use of logistic regression and artificial neural networks with different sampling strategies for the preparation of landslide susceptibility maps. *Engineering Geology* 97, 171–191.
- Neuhauser, B., Terhorst, B., 2007. Landslide susceptibility assessment using “weights-of-evidence” applied to a study area at the Jurassic escarpment (SW-Germany). *Geomorphology* 86, 12–24.
- Ohlmacher, G.C., Davis, J.C., 2003. Using multiple logistic regression and GIS technology to predict landslide hazard in northeast Kansas, USA. *Engineering Geology* 69, 331–343.
- Picarelli, L., Oboni, F., Evans, S.G., Mostyn, G., Fell, R., 2005. Hazard characterization and quantification. In: Hungr, O., Fell, R., Couture, R., Eberhardt, E. (Eds.), *Landslide Risk Management*. Taylor and Francis, London, pp. 27–61.
- Seshagiri, D.N., Badrinarayanan, B., 1982. The Nilgiri landslides. Geological Survey of India. Misc. Pub. No 57.
- Soeters, R., van Westen, C.J., 1996. Slope instability recognition, analysis and zonation. In: Turner, A.K., Schuster, R.L. (Eds.), *Landslide Investigation and Mitigation*, National Research Council, Transportation Research Board Special Report 247, pp. 129–177.
- Stark, C.P., Hovius, N., 2001. The characterization of landslide size distributions. *Geophysics Research Letters* 28 (6), 1091–1094.
- Suzen, M.L., Doyuran, V., 2004. A comparison of the GIS based landslide susceptibility assessment methods: multivariate versus bivariate. *Environmental Geology* 45, 665–679.
- van Westen, C.J., Rengers, N., Soeters, R., 2003. Use of geomorphological information in indirect landslide susceptibility assessment. *Natural Hazards* 30 (3), 399–419.
- van Westen, C.J., Asch, T.W.J., Soeters, R., 2006. Landslide hazard and risk zonation — why is it still so difficult? *Bulletin of Engineering Geology and the Environment* 65, 67–184.
- van Westen, C.J., Castellanos, E., Kuriakose, S.K., 2008. Spatial data for landslide susceptibility, hazard, and vulnerability assessment: an overview. *Engineering Geology* 102, 112–131.
- Varnes, D.J., 1984. *Landslide Hazard Zonation: A Review of Principles and Practice*. UNESCO, Daramtiere, Paris, p. 61.
- Venables, W.N., Smith, D.M., R Development Core Team, 2007. *An Introduction to R: A Programming Environment for Data Analysis and Graphics*. Version 2.5.1 (2007-06-27), 'R' Help File.
- Yesilnacar, E., Topal, T., 2005. Landslide susceptibility mapping: a comparison of logistic regression and neural networks methods in a medium scale study, Hendek region (Turkey). *Engineering Geology* 79, 251–266.
- Zeze, J.L., Reis, E., Garcia, R., Oliveira, S., Rodrigues, M.L., Vieira, G., Ferreira, A.B., 2004. Integration of spatial and temporal data for the definition of different landslide hazard scenarios in the area north of Lisbon (Portugal). *Natural Hazards and Earth System Sciences* 4, 133–146.
- Zeze, J.L., Trigo, R.M., Trig, I.F., 2005. Shallow and deep landslides induced by rainfall in the Lisbon region (Portugal): assessment of relationships with the North Atlantic Oscillation. *Natural Hazard and Earth System Sciences* 5, 331–344.
- Zweig, M.H., Campbell, G., 1993. Receiver operator characteristic plots: a fundamental evaluation tool in clinical medicine. *Clinical Chemistry* 39 (4), 561–577.